https://doi.org/10.15407/ujpe71.1.28

A. JUMABAEV,[1] H. HUSHVAKTOV,[1] A. ABSANOV,[1] I. DOROSHENKO,[1,2]
B. KHUDAYKULOV,[1] L. DJUMANOV,[1] Z. ERNAZAROV [1]

[1] Sharof Rashidov Samarkand State University
*(15, University Blvd., Samarkand 703004, Uzbekistan; e-mail: abduvakhidj@gmail.com)*
[2] Taras Shevchenko National University of Kyiv
*(64/13, Volodymyrska Str., Kyiv 01601, Ukraine; e-mail: dori11@knu.ua)*

# INSIGHTS INTO AMYL ACETATE–CHLOROFORM INTERACTIONS: VIBRATIONAL SPECTROSCOPY AND QUANTUM TOPOLOGY STUDY

*This study employs density functional theory (DFT) and Raman spectroscopy to examine the spectrum manifestation of the interaction between amyl acetate (AmAc) and chloroform. A red shift in the C=O stretching vibration band was seen when the concentration of AmAc in the solution decreased, suggesting that intermolecular hydrogen bonds were forming in the solution. At the DFT/B3LYP/6-311++G(d, p) level, the optimal geometry of the complexes consisting of AmAc monomers, dimers, and chloroform molecules was determined. Topological analysis methods such as AIM, RDG, NCI, ELF, and LOL were used to gather information regarding the existence and characteristics of H-bonds (including C–H···O). Important insights on intermolecular interactions in solution were provided by the discovery of the connection between the C=O stretching vibrational bands and the creation of molecular clusters.*

*Keywords*: Raman spectroscopy, hydrogen bonding, amyl acetate, chloroform, molecular electrostatic potential (MEP) surface.

## 1. Introduction

Determining the internal mechanisms of chemical and biological processes required for the emergence of life requires a thorough examination of the nature of interactions between atoms and molecules as well as a thorough study of their scientific foundations. This analysis forms the basis for the creation of new theories and useful methods [1–5]. The molecular dynamics and structure of pure and mixed liquids have received considerable attention recently, and aspects remain the subject of ongoing debate [6].

The formation of noncovalent interactions, particularly hydrogen (H) bonds, occurs on picosecond timescales and is crucial for both molecular structure and energetic properties. H-bonding is frequently studied using Raman and infrared spectroscopy methods, particularly when elucidating the micromolecular dynamics of chemical and biological systems [7–9].

Interactions between solvent and the solute molecules have been widely studied in the field of chemical physics, and it has been established that these interactions play an important role in determining the chemical and physical properties of the solution [10]. To understand the processes of the sol-

Citation: Jumabaev A., Hushvaktov H., Absanov A., Doroshenko I., Khudaykulov B., Djumanov L., Ernazarov Z. Insights into amyl acetate–chloroform interactions: vibrational spectroscopy and quantum topology study. *Ukr. J. Phys.* **71**, No. 1, 28 (2026). https://doi.org/10.15407/ujpe71.1.28.

vent–solute interactions at the molecular level, it is necessary to have a detailed knowledge of the dynamic properties of the interaction processes. Such insight enables a clearer understanding of the nature of the interactions at the molecular level. As a result, knowledge about the relationship between the solute and the solvent and their interaction will expand, which will serve as an important basis for modeling and predicting various chemical and physical processes [11].

Amyl acetate (AmAc) has been studied by many scientists due to the presence of two electronegative moieties: ether-oxygen and carbon-oxygen bonding [12–14]. The C=O group is an ideal representative for protein analysis, and the C=O stretching vibration frequency is typically observed near 1700 $cm^{-1}$ [15]. The structure of the AmAc molecule is an ester, which is formed by the bonding of an acetyl group ($CH_3CO$–) and an ethyl group (–$(CH_2)_4CH_3$) via an oxygen. Any information about the structure and bonding characteristics, electronic structure, and geometry of this AmAc molecule is of great importance in the chemistry and physics of liquids [13].

The aim of this work is to elucidate the geometric and physical structure of AmAc-chloroform solutions. In this work, the intermolecular interactions in the pure AmAc and its chloroform solutions are investigated using Raman spectroscopy and quantum chemical calculations, with particular emphasis on the C=O spectral region. Also, DFT calculations of the molecules, Mulliken atomic charge distribution, topological analyses (atoms in molecules (AIM) analysis, reduced density gradient (RDG), noncovalent interaction (NCI), electron localization functions (ELF) and localized orbital locator (LOL)) were performed.

## 2. Experimental and Theoretical Methods

### *2.1. Experimental method*

Raman spectra of neat AmAc and its chloroform solutions of AmAc were recorded at room temperature on a Renishaw Invia Raman spectrometer equipped with a diffraction grating with a 1200 lines/mm diffraction grating. Excitation was provided by an argon laser with a wavelength of 532 nm and a power of 50 mW. The scattered light was detected using a standard Renishaw CCD Camera detector.

### *2.2. Computational Method*

All calculations were performed within the framework of density functional theory (DFT) method in Gaussian software package 09W [16]. The molecular structure of AmAc and chloroform was calculated using the DFT/6-311++G(d, p) method and the B3LYP (Becke-3-Li-Yang-Parr) hybrid functional [17–18]. The spectra were generated and visualized using with Origin 8.5 [19]. The geometric structure of the molecule was visualized using GaussView 6 [20] and VMD [21]. The topological parameters of AIM, NCI, RDG, ELF and LOL were calculated using Multiwfn 3.8 (64-bit) [22].

## 3. Results and Discussion

### *3.1. Raman spectra of AmAc-chloroform solution*

Figure 1 shows the Raman spectra in the region of the C=O stretching vibrations bands involved in the intermolecular interaction between AmAc and chloroform in the solution. In the neat state, the maximum of the C=O vibration band corresponds to $\nu =$ $= 1741$ $cm^{-1}$. As the AmAc concentration decreases, the maximum of the band shifts to a lower frequency. When the AmAc concentration in the solution is 0.9 and 0.8 m.f. (mole fraction), the frequency of the C=O stretching band corresponds to $\nu = 1740$ $cm^{-1}$ and $\nu = 1739$ $cm^{-1}$, which is shifted to a lower fre-

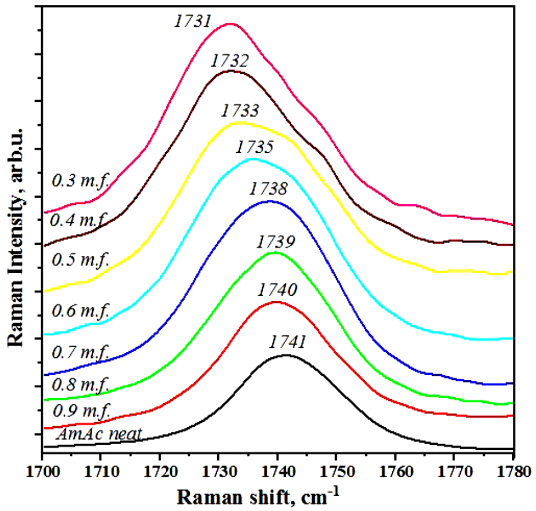


***Fig. 1.*** Raman spectra in the region of C=O stretching vibration bands in AmAc and its solution in chloroform (in mole fraction (m.f.))

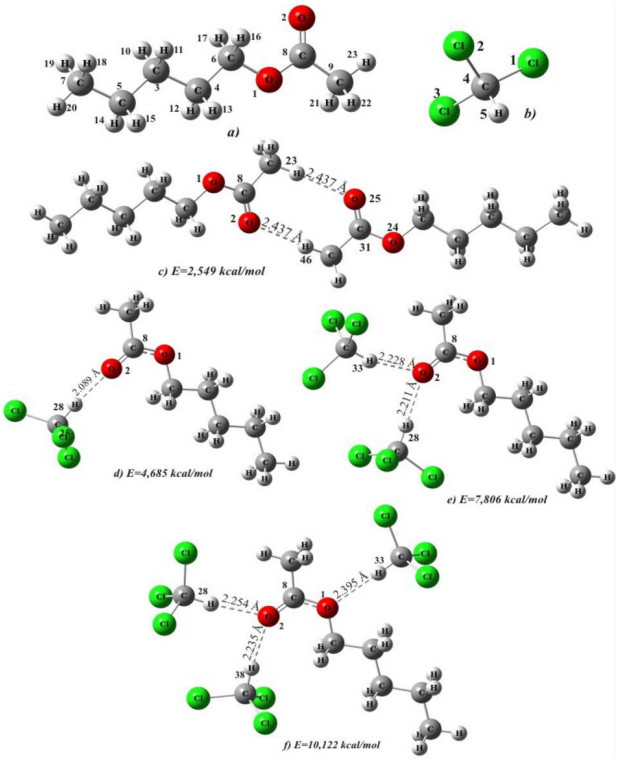


***Fig. 2.*** Optimal geometry of AmAc-chloroform complexes

quency respectively by 1 and 2 $cm^{-1}$ compared to the neat state. As the amount of AmAc in the solution decreases, the frequency of the C=O stretching vibration band decreases. When the amount of AmAc is at least 0.3 m.f., the band peak position shifts to $\nu = 1731$ $cm^{-1}$ i.e. by 10 $cm^{-1}$ compared to the neat state. One of the main reasons for the shift of the band maximum is intermolecular hydrogen bonding [23–24]. As the concentration increases, the band corresponding to the C=O stretching vibration shifts to a lower frequency.

### *3.2. Geometry optimization of AmAc-chloroform complexes*

Calculations show that AmAc can exist in several aggregated forms. Figure 2, *a* shows the calculated geometry of AmAc monomer. Figure 2, *c* shows the monomer of AmAc. Figure 2, *c* shows the dimer of AmAc molecules, and during dimer formation, the $O^2$ atom in the C=O group of the first molecule forms a C–H ... O H-bond with a H ... O distance of 2.437 Å with the $H^{46}$ atom in the C–H group of the neighboring molecule, and the $H^{23}$ atom in the C–H group of the first molecule also forms a C–H ... O H-bond with a H ... O distance of 2.437 Å with the $O^{25}$ atom in the C=O group of the neighboring molecule.

Figure 2, *d* shows the AmAc–1chloroform complex. In this complex, a cluster is formed due to the H-bond (bond length 2.089 Å) between the $O^2$ atom of AmAc and the $H^{28}$ atom of the chloroform molecule. Figure 2, *e* shows the complex of AmAc with two chloroform molecules, where the $O^2$ atom of AmAc is bonded to hydrogen atoms of both chloroforms, with a H-bond between the $H^{28}$ atoms of the first chloroform molecule with a bond length of 2.211 Å and a H-bond with the $H^{33}$ atom of the second chloroform molecule with a bond length of 2.228 Å. In the complex of AmAc with 3 chloroform molecules (Fig. 2, *f*), the $O^2$ oxygen atom of the C=O group of AmAc participates in H-bonding with two chloroform molecules (bond lengths $O^2$ ... $H^{28}$ – 2.254 Å, $O^2$ ... $H^{38}$ – 2.235 Å). In this complex, the hydrogen atoms of two chloroforms form a hydrogen bond through the $O^2$ atom in the C=O group of AmAc, while the hydrogen atom of the third chloroform forms a complex through the second $O^1$ atom in the C–O–C group of AmAc, with a bond length of $O^1$ ... $H^{33}$ – 2.395 Å. From this, it can be said that the AmAc molecule participates in mainly weak intermolecular interactions with chloroform molecules.

### *3.3. Calculated of Raman spectra for AmAc-chloroform complexes*

Figure 3 shows the calculated Raman spectra in the region of the C=O stretching vibration for the AmAc monomer and its complex with chloroform. The maximum of the C=O stretching band for the AmAc monomer is at 1790 $cm^{-1}$ (Fig. 3, *a*). In Figure 3, *b*, the maximum of this band for the AmAc-chloroform dimer is at 1772 $cm^{-1}$, shifted by 18 $cm^{-1}$ towards lower frequencies relative to the monomer. This shift is due to the hydrogen atom of chloroform being bonded to the $O^2$ atom in the C=O group of AmAc. In the AmAc–chloroform complex, when the number of chloroform molecules reaches two, the C=O stretching band is at 1747 $cm^{-1}$, which is shifted to a lower frequency by 43 $cm^{-1}$ compared to the monomer. This is due to the hydrogen atoms of both chloroform molecules forming H-

bond through the $O^2$ atom in the C=O group of AmAc (Fig. 3, *c*). When the number of chloroform molecules reaches three, the C=O stretching band is at 1755 $cm^{-1}$, which is shifted to a lower frequency by 35 $cm^{-1}$ compared to the monomer. This is due to the hydrogen atoms of two chloroforms forming a hydrogen bond through the $O^2$ atom in the C=O group of AmAc, while the hydrogen atom of the third chloroform is hydrogen bonded through the second $O^1$ atom in the C–O–C group of AmAc. Therefore, as the number of chloroform molecules in the AmAc–chloroform complex increases, the C=O vibration frequency decreases. This is consistent with the shift of the stretching vibration band to a lower frequency in hydrogen-bonding theory [23].

### *3.4. Molecular electrostatic potential (MEP)*

Molecular electrostatic potential (MEP) or molecular potential surface map is an important tool for visualizing the charge distribution in AmAc–chloroform complexes and for studying electrophilic, nucleophilic reactions and bonding, which are charge-dependent parameters [25]. Another purpose of finding the MEP is to identify the reactive parts of the molecule. Figure 4 depicts the MEP using a color scale in which the electrostatic potential generally increasing in the following order: red, orange, yellow, green and blue [26].

The MEP in the range of $t(-5.202\times10^{-2} \ldots 5.202 \times \times 10^{-2})$ eV shows that the oxygen atoms in the C=O groups of AmAc monomer have a negative potential. The red color reflects the electrophilic region that determines the largest negative charge of the molecule. The blue color around $CH_3$ represents the nucleophilic positive charge part, the yellow color around the C–O–C group represents a slightly electron-rich region, and the green color represents zero potential (Fig. 4) [27]. When the MEP map in the range of $(-4.469 \times 10^{-2} \ldots 4.469 \times 10^{-2})$ eV is viewed for the AmAc dimer complex, the red color around the oxygen atom in the C=O group of AmAc has changed to yellow, i.e. the potential of this region has decreased. The potential around the oxygen in the O–C–O group of AmAc also shows a slightly electron-rich region, which is yellow. The MEP map for the AmAc–1 Chloroform complex was observed in the range of $(-2.481 \times 10^{-2} \ldots 2.481 \times 10^{-2})$ eV,

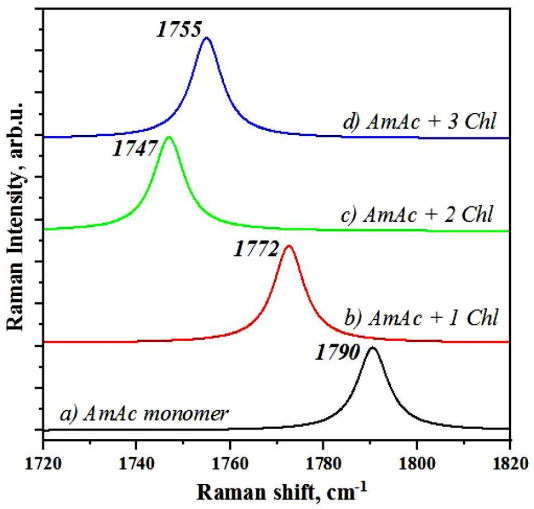


***Fig. 3.*** Raman spectra in the region of the C=O stretching vibration for AmAc–chloroform complexes

where the red color around the oxygen atom of the C=O group of AmAc changed to yellow, indicating a decrease in the potential in this region. The MEP calculated for AmAc–2 Chloroform and AmAc–3 Chloroform were $(-2.724\times10^{-2} \ldots 2.224\times10^{-2})$ eV and $(-3.319 \times 10^{-2} \ldots 3.319 \times 10^{-2})$ eV, respectively, with the surrounding O atoms changing from red to yellow as the amount of chloroform molecules in the complex increased. Figure 3 shows the interaction of AmAc with chloroform molecules through weak interactions, which may explain the red shift of the bands in the spectrum.

### *3.5. Frontier Molecular Orbital (FMO) Analysis*

The electronic properties and reactivity of molecules can be rationalized by analyzing their frontier molecular orbitals (FMO), i.e. the highest occupied molecular orbital (HOMO) and the lowest unoccupied molecular orbital (LUMO). These orbitals play a central role in various chemical processes, especially those involving electron transfer. The HOMO is important for electron-donating or nucleophilic reactions and can easily participate in oxidation or nucleophilic reactions [28]. In contrast, the LUMO is the next orbital that electrons can occupy, representing an electron-occupied or empty molecular orbital. Molecules with low LUMO energies are generally good electron acceptors and can participate in electrophilic

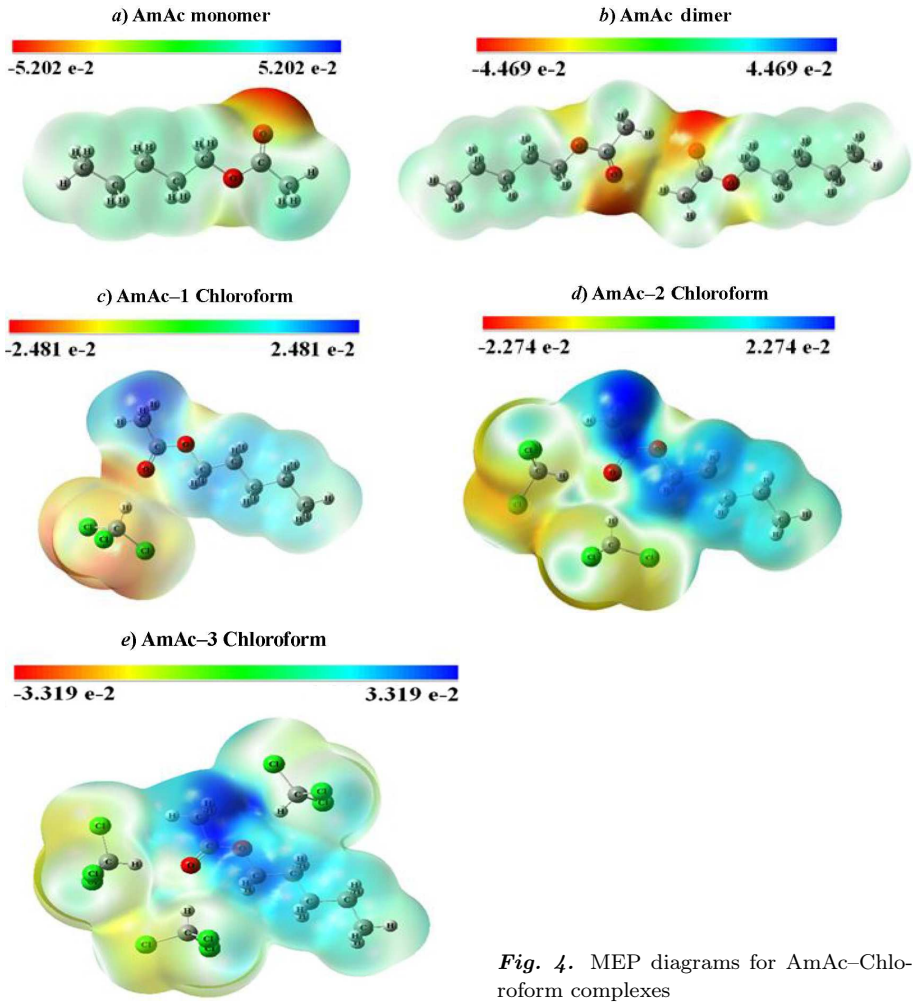


***Fig. 4.*** MEP diagrams for AmAc–Chloroform complexes

*Table 1.* **Thermodynamic and FMO related parameters of AmAc–Chloroform**

| Parameters | AmAc monomer | AmAc dimer | AmAc– 1 Chloroform | AmAc– 2 Chloroform | AmAc– 3 Chloroform |
|---|---|---|---|---|---|
| Dipole moment, $\mu$ (Debye) | 2.251 | 0.327 | 4.44 | 4.891 | 3.238 |
| Total energy (Thermal) (kcal/mol) | 134.344 | 270.548 | 150.878 | 167.392 | 185.743 |
| Zero-point vibrational energy (kcal/mol) | 127.081 | 254.715 | 139.837 | 152.651 | 165.609 |
| $E_{\mathrm{HOMO}}$ (kcal/mol) | –176.686 | –173.994 | –187.397 | –192.699 | –197.067 |
| $E_{\mathrm{LUMO}}$ (kcal/mol) | –7.003 | –6.193 | –25.389 | –37.048 | –38.315 |
| $E_{\mathrm{LUMO}} - E_{\mathrm{HOMO}}$ | 169.683 | 167.801 | 162.009 | 155.652 | 158.752 |
| Global hardness, $\eta = (E_{\mathrm{LUMO}} - E_{\mathrm{HOMO}})$ | 84.842 | 83.901 | 81.004 | 77.826 | 79.376 |
| Chemical potential, $\mu = (E_{\mathrm{LUMO}} + E_{\mathrm{HOMO}})$ | –91.845 | –90.094 | –106.393 | –114.874 | –117.691 |
| IP $= -E_{\mathrm{HOMO}}$ | 176.686 | 173.994 | 187.397 | 192.699 | 197.067 |
| EA $= -E_{\mathrm{LUMO}}$ | 7.003 | 6.193 | 25.389 | 37.048 | 38.315 |
| Electrophilicity index, $\omega = \mu^2/2\eta$ | 49.713 | 48.372 | 69.869 | 84.779 | 87.251 |

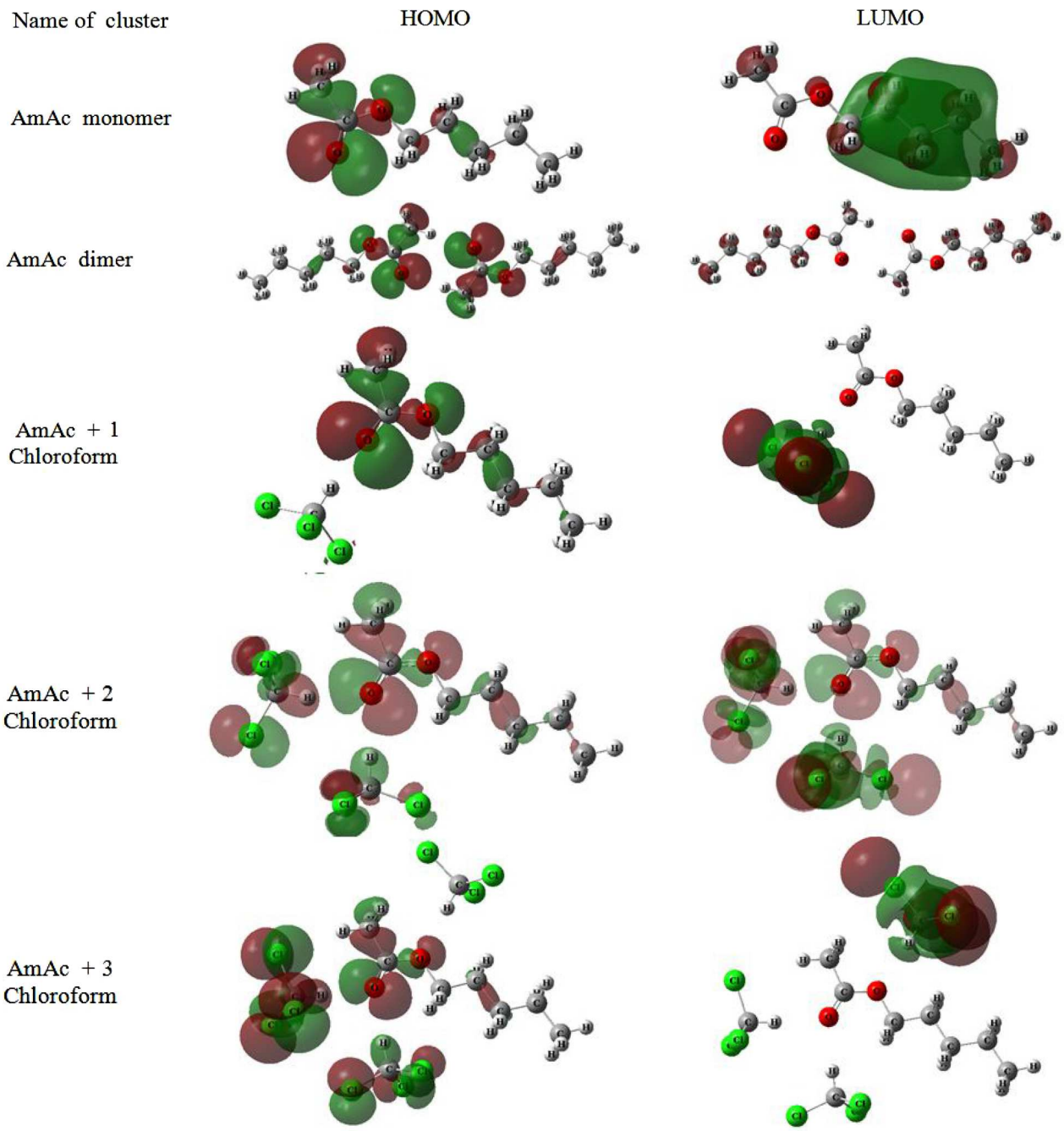


***Fig. 5.*** Frontier molecular orbital diagram of AmAc–Chloform complexes

reactions [29]. Figure 5 presents the HOMO–LUMO visualization. Table 1 lists the thermodynamic and chemical parameters of AmAc-chloroform complexes and the parameters determined by the HOMO and LUMO energy difference. According to Table 1, the dipole moment for the AmAc–1 Chloroform complex is larger than that of the monomer.

The vibrational energy and the HOMO–LUMO energy difference are the largest for the AmAc–1 Chloroform complexes (162.009 kcal/mol). For the

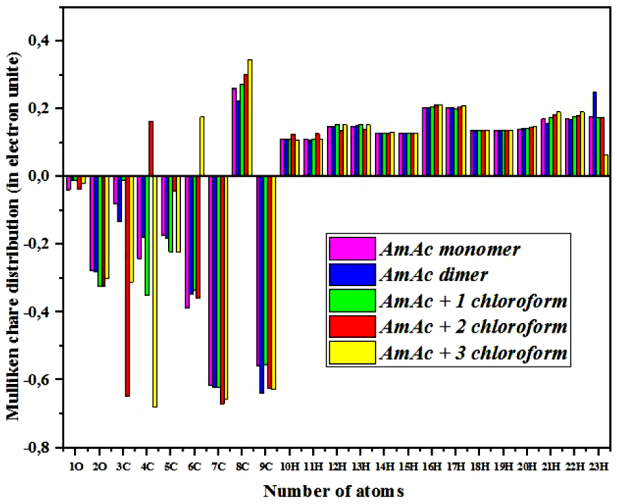


***Fig. 6.*** Mulliken charge distribution of AmAc–chloroform complexes

other complexes the values are: 169.683 kcal/mol (AmAc monomer), 167.801 kcal/mol (AmAc dimer), 162.009 kcal/mol (AmAc–1 Chloroform), 155.652 kcal/mol (AmAc–2 Chloroform), 158.752 kcal/mol (AmAc–3 Chloroform), and the largest value for AmAc–1 Chloroform. The ionization potential values are 176.686 kcal/mol (AmAc monomer), 173.994 kcal/mol (AmAc dimer), 187.397 kcal/mol (AmAc–1 Chloroform), 192.699 kcal/mol (AmAc–2 Chloroform), and 197.067 kcal/mol (AmAc–3 Chloroform). The electrophilicity index of 87.251 kcal/mol is the largest for the AmAc–3 Chloroform complex.

### *3.6. Mulliken charge of AmAc–Chloroform complexes*

The analysis of the Mulliken atomic charge using quantum chemical calculations plays an important role in explaining the molecular behavior of complexes, as atomic charges affect a number of molecular properties, including electronic structure, reactivity, dipole moment, polarization, and vibrational spectra. Figure 6 shows a graphical representation of the Mulliken charge distribution for the complexes. In the AmAc and AmAc–1 Chloroform complexes, all hydrogen atoms are positively charged, whereas oxygen atoms are negatively charged.

During the formation of the complex, the electron density at the carbon atom of the C=O group increases sharply due to the charge exchange between hydrogen and oxygen atoms. The charge of the carbon atom changes from $0.262e$ in the monomer to $0.225e$ (AmAc–1 Chloroform). Similarly, the charge of the oxygen atom ($O^2$) changes from $-0.276e$ to $-0.325e$ (AmAc–1 Chloroform). Such changes in charge distribution lead to an increase in the bond length of the carboxyl group, which leads to changes in the frequencies at different solvent concentrations.

If we look at the charges of the atoms participating in the interaction between AmAc and chloroform, the charge modulus of the $C^8$ and $H^{21}$ atoms has increased. The charge modulus of the $O^3$ and $C^7$ atoms has decreased. It can be seen from Figure 6 that the charge distribution for the AmAc–2 Chloroform and AmAc–3 Chloroform complexes has also partially changed, and this change is significant for the atoms participating in the interaction.

### *3.7. Atoms in molecules (AIM) analysis for AmAc–Chloroform complexes*

Atoms in molecules (AIM) analysis is widely used to determine noncovalent interactions in molecular systems [30]. Owing to the electron density, a bond path appears between two interacting atoms, which creates critical points (CPs) in the electron density. At such points, its electron density gradient disappears. The presence of H-bonds or other interactions in molecular complexes is confirmed by topological analysis of the electron density. Figure 7 shows the topological parameters for the AmAc dimer, AmAc–1 Chloroform and AmAc–2 Chloroform complexes: electron density $\rho(r)$, electron density Laplacian $\nabla^2\rho(r)$, energy density $H(r)$, and the Lagrangian kinetic energy density $G(r)$, and potential energy density $V(r)$ in BCPs, which provide detailed information about the nature of the interaction (Table 2). According to Table 2, the Laplacian of the electron density ($\nabla^2\rho(r)$) for the AmAc dimer, AmAc–1 Chloroform, AmAc–2 Chloroform, and AmAc–3 Chloroform complexes takes positive values in the range of 0.0295 a.u. and 0.0294 a.u. (AmAc dimer), 0.0689 a.u. (AmAc–1 Chloroform), 0.0483 a.u. and 0.0500 a.u. (AmAc–2 Chloroform), 0.0326 a.u., 0.0448 a.u., and 0.0471 a.u. (AmAc–3 Chloroform), respectively. Similarly, the energy density values $H(r)$ were found to be positive with the values of 0.0010 a.u. and 0.0010 a.u. (AmAc dimer), 0.0031 a.u. (AmAc–1 Chloroform), 0.0016 a.u. and 0.0020 a.u. (AmAc–2 Chloroform), 0.0011 a.u.,

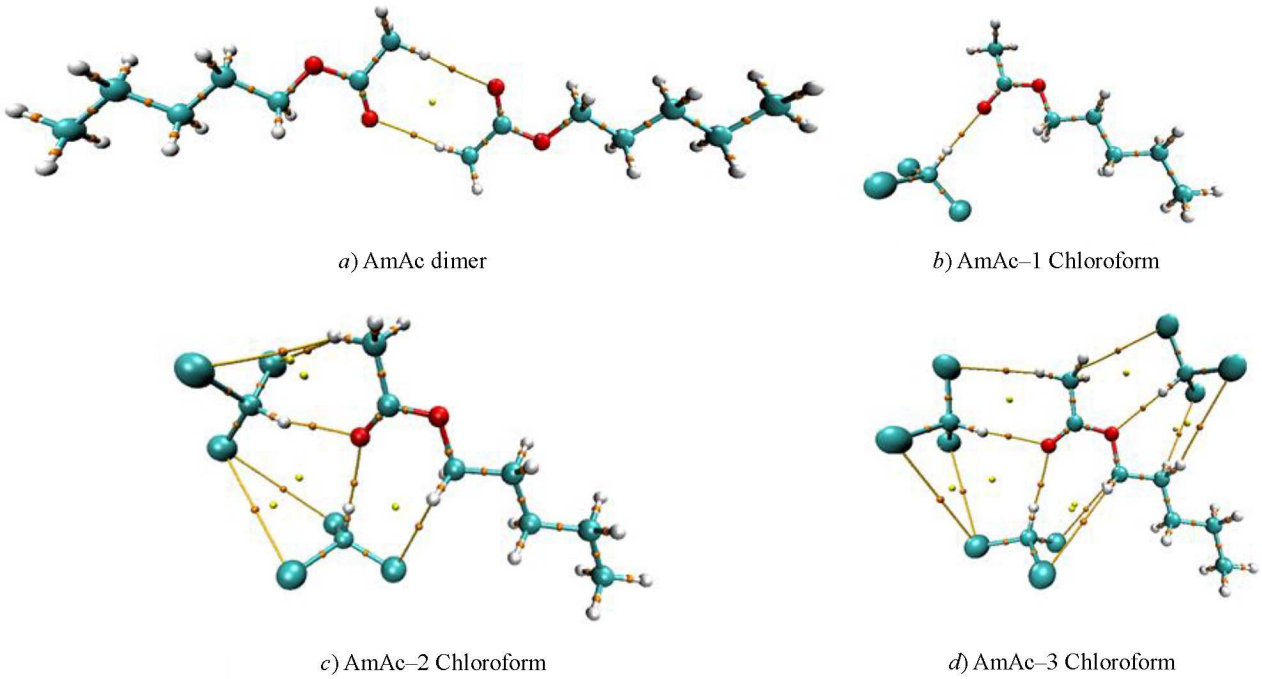


***Fig. 7.*** The molecular diagrams of title complexes

*Table 2.* **Topological parameters of AmAc, AmAc-chloroform (Chl) complexes**

| Cluster | X(H)-bonds | Bond length $r$, Å | Density of all electrons $\rho(r)$ | Lagrangian kinetic energy $G(r)$ | Potential energy density $V(r)$ | Energy density $H(r)$ | Laplacian of electron density $\nabla^2\rho(r)$ | Bond energy $E_{\text{int}} \approx -V(r)/2$, kcal/mol |
|---|---|---|---|---|---|---|---|---|
| AmAc dimer | 2(O)···46(H) | 2.43684 | 0.0094 | 0.0063 | –0.0053 | 0.0010 | 0.0295 | 1.66 |
| | 23(H)···25(O) | 2.43738 | 0.0094 | 0.0063 | –0.0053 | 0.0010 | 0.0294 | 1.66 |
| AmAc–1 Chl | 2(O)···28(H) | 2.08911 | 0.0165 | 0.0141 | –0.0110 | 0.0031 | 0.0689 | 3.45 |
| AmAc–2 Chl | 2(O)···33(H) | 2.22892 | 0.0146 | 0.0104 | –0.0088 | 0.0016 | 0.0483 | 2.76 |
| | 2(O)···28(H) | 2.21128 | 0.0138 | 0.0105 | –0.0085 | 0.0020 | 0.0500 | 2.67 |
| AmAc–3 Chl | 1(O)···33(H) | 2.39546 | 0.0102 | 0.0070 | –0.0059 | 0.0011 | 0.0326 | 1.85 |
| | 2(O)···28(H) | 2.25436 | 0.0136 | 0.0096 | –0.0081 | 0.0015 | 0.0448 | 2.54 |
| | 2(O)···38(H) | 2.23572 | 0.0133 | 0.0099 | –0.0081 | 0.0018 | 0.0471 | 2.54 |

0.0015 a.u. and 0.0018 a.u. (AmAc–3 Chloroform), respectively. This supports the existence of weak H-bonds between the complexes [31]. The formula $E_{\text{int}} = V(r)/2$ was used to calculate the binding energy. Here, $V(r)$ is the potential energy density at the CPs of the bond. If the energy density value at the CPs is negative (HBCPs $< 0$), the bond is covalent, and if it is positive (HBCPs $> 0$), the bond is electrostatic. According to Table 2, all complexes are formed through weak H-bonding.

### *3.8. Noncovalent interaction (NCI) and reduced density gradient (RDG)*

The NCI index is used to characterize intermolecular interactions and assess the nature of weak interactions. It is based on the reduced density gradient (RDG) and provides additional information in studying of noncovalent interactions. The reduced density gradient (RDG) is a fundamental dimensionless quantity consisting of the electron density and its first

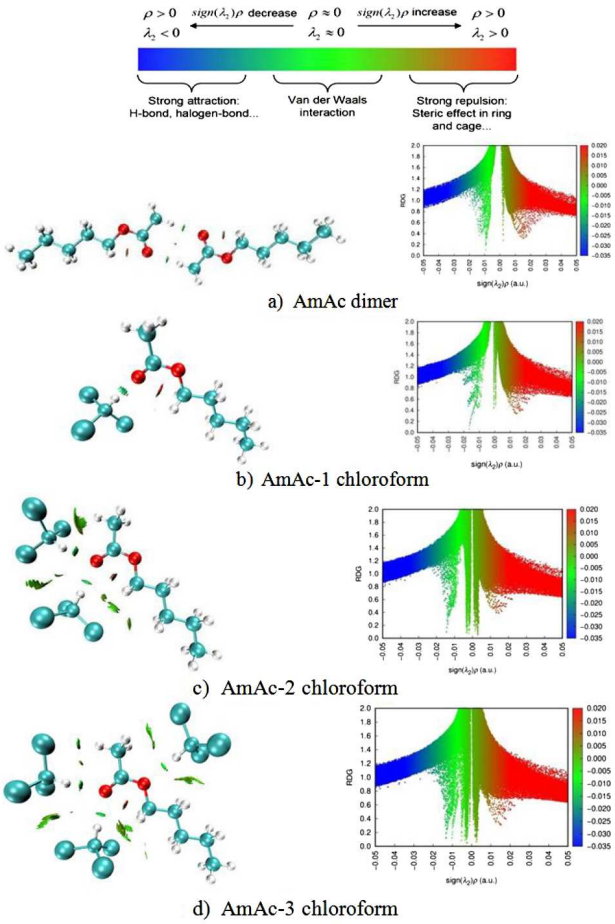


***Fig. 8.*** NCI and RDG analyses for title complexes

derivative, and given by Eq. (1) [32]:

$$\mathrm{RDG}(r) = \frac{1}{2(3\pi^2)^{1/3}} \frac{|\nabla\rho(r)|}{\rho(r)^{4/3}}. \qquad (1)$$

In molecular systems, blue represents attraction and red represents repulsion. The parameter $\mathrm{sign}(\lambda_2)\rho$ is important in predicting the nature of the interaction: for example, $\mathrm{sign}(\lambda_2)\rho < 0$ represents attraction between bonded atoms, while $\mathrm{sign}(\lambda_2)\rho > 0$ represents repulsion between unbonded atoms.

The RDG scattering plots of the complexes are presented on the right side of Figure 8. According to the results, in the AmAc dimer, AmAc–1 Chloroform, AmAc–2 Chloroform and AmAc–3 Chloroform complexes, the green circle atoms between AmAc and chloroform atoms form a weak H-bond of the C=O···H type, and this effect can be compared to the nature of the van der Waals interaction. It can also

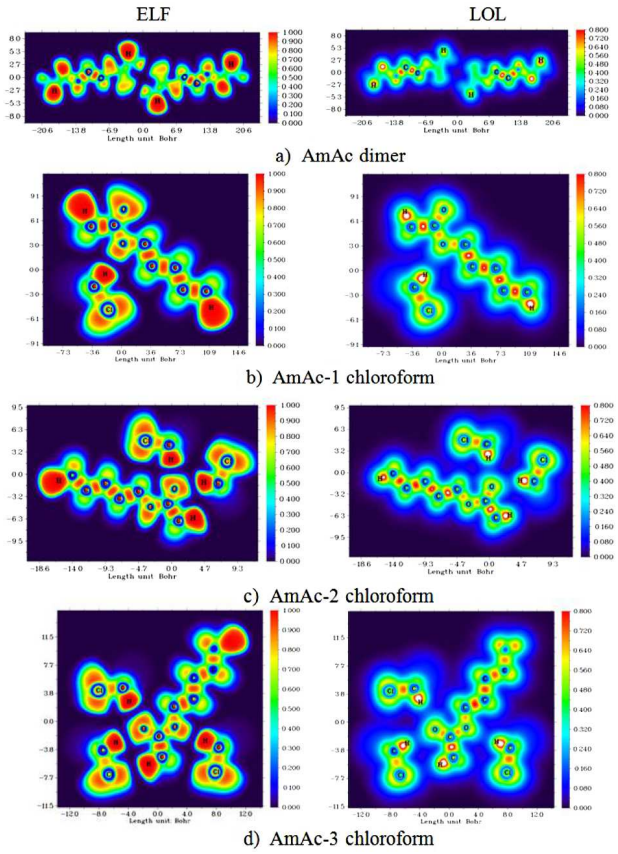


***Fig. 9.*** ELF and LOL maps of title complexes

be seen from the RDG scatter plots on the right side of Figure 8 that the scattering mainly occurs in the range of $\mathrm{sign}(\lambda_2)\rho$ values from –0.02 to 0.00, which represents the van der Waals interaction (Figs 8, *a*–*c*). In the AmAc–1 Chloroform complexes, the circle between the oxygen atom of AmAc and the hydrogen atoms of chloroform is partially colored blue, which is considered to be the effect of weak H-bonding. This is supported by the blue scattering ($\mathrm{sign}(\lambda_2)\rho$ value corresponding to –0.02) observed in the right part of Fig. 8, *b* and in the RDG scatter plot. In general, the formation of hydrogen bonds in the form of C=O···H between AmAc and chloroform molecules is consistent with the nature of the Van der Waals interaction, and due to this effect, red shift in the C=O vibrational band was observed.

### *3.9. ELF and LOL analyses*

Electron localization function (ELF) and localized orbital locator (LOL) analyses are widely used to de-

scribe chemical bonding in atomic and molecular systems and to identify regions where electrons are located [32]. While ELF describes the pairwise electron density, LOL describes the maximum localized orbitals that overlap each other due to the gradient of orbitals. Figure 9 shows the ELF and LOL color maps for the AmAc dimer (*a*), AmAc–1 Chloroform (*b*), AmAc–2 Chloroform (*c*), and AmAc–3 Chloroform (*d*) complexes. The color values on the y-axis range from blue to red, with ELF values ranging ranging from 0 to 1.0 and LOL numbers from 0 to 0.8. Both ELF and LOL have interval scales, representing bonded and unbonded local electron zones ranging from 0.5 to 1.0.

Delocalized electrons are indicated by the region with a value below 0.5. Red and orange colors indicate high electron localization. The region between the inner and valence shells is indicated by the blue circle. Color shades of the ELF and LOL maps: red has the highest value around hydrogen atoms, indicating the presence of both bonded and unbonded electrons. The red color area with high ELF or LOL values shown around hydrogen atoms indicates a lone pair of electrons due to covalent bonding or a high localization of electrons due to the presence of a nuclear shell in this area.

## 4. Conclusion

Spectroscopic and quantum chemical studies of amyl acetate (AmAc) and its solutions in chloroform have shown that a decrease in the frequency of the C=O stretching vibration band in solution is due to the formation of intermolecular H-bonds. Calculations revealed the presence of C–H···O H-bonds between AmAc and chloroform molecules. The geometry and energy of the resulting complexes were studied using DFT calculations performed at the B3LYP/6-311++G(d,p) level. AIM, RDG, NCI, ELF, and LOL analyses were used to determine the nature of these interactions. The results obtained provide an important theoretical basis for understanding the spectroscopic behavior of AmAc in solution, cluster formation, and solution structure. This can be used in the future to model the interactions of other organic solvents.

*This work was supported by Project No. FZ20200929385 of the Ministry of Higher Education, Science and Innovation of the Republic of Uzbekistan.*

1. H. Hushvaktov, B. Khudaykulov, A. Jumabaev, I. Doroshenko, A. Absanov, G. Murodov. Study of formamide molecular clusters by Raman spectroscopy and quantum chemical calculations. *Mol. Cryst. Liq. Cryst.* **749**, 1 (2022).
2. I.G. Kaplan. *Intermolecular Interactions: Physical Picture, Computational Methods and Model Potentials* (John Wiley and Sons, 2006).
3. A. Jumabaev, B. Khudaykulov, I. Doroshenko, H. Hushvaktov, A. Absanov. Raman and ab initio study of intermolecular interactions in aniline. *Vib. Spectrosc.* **122**, 103422 (2022).
4. H.A. Hushvaktov, F.H. Tukhvatullin, A. Jumabaev, U.N. Tashkenbaev, A.A. Absanov, B.G. Hudoyberdiev, B. Kuyliev. Raman spectra and ab initio calculation of a structure of aqueous solutions of methanol. *J. Mol. Struct.* **1131**, 25 (2017).
5. A. Jumabaev, A. Absanov, Z. Ernazarov, A. Shodiyev, S. Umarov. Raman spectra and ab initio calculation analysis of intermolecular interactions in ethylacetate. *SamSU Bulletin. Bull.* **3,** 132 (2023).
6. B.B. Xudaykulov. Study of molecular interactions in aniline and its aqueous solutions: experiment and calculations. *Uzbek Phys. J.* **24**, 2 (2022).
7. B. Khudaykulov, A. Norkulov, U. Holikulov, A. Absanov, I. Doroshenko, A. Jumabaev, Raman and DFT study of noncovalent interactions in liquid benzophenone and its solutions. *Low Temp. Phys.* **51**, 2 (2025).
8. A. Jumabaev, A.A. Absanov, B.B. Khudaykulov, Z.I. Ernazarov. Investigation of intermolecular interactions in butyl acetate using vibrational spectroscopy and nonempirical calculations. *Uzbek Phys. J.* **25**, 4 (2023).
9. A. Jumabaev, H. Hushvaktov, A. Absanov, I. Doroshenko, B. Khudaykulov. Experimental and computational analysis of C–N and C–H stretching bands in acetonitrile solutions. *Low Temp. Phys.* **51**, 2 (2025).
10. A. Ghosh, J. Wang, Y.S. Moroz, I.V. Korendovych, M. Zanni, W.F. DeGrado, R.M. Hochstrasser. 2D IR spectroscopy reveals the role of water in the binding of channel-blocking drugs to the influenza M2 channel. *J. Chem. Phys.* **140**, 23 (2014).
11. L. Chuntonov, I.M. Pazos, J. Ma, F. Gai. Kinetics of exchange between zero, one, and two-hydrogen-bonded states of methyl and ethyl acetate in methanol. *J. Phys. Chem. B* **119**, 4512 (2015).
12. J.Y. Lai, K.C. Lin, A. Violi. Biodiesel combustion: Advances in chemical kinetic modeling. *Prog. Energy Combust. Sci.* **37**, 1 (2011).
13. A. Mahendraprabu, T. Sangeetha, P.P. Kannan, N.K. Karthick, A.C. Kumbharkhane, G. Arivazhagan. Hydrogen bond interactions of ethyl acetate with methyl Cellosolve: FTIR spectroscopic and dielectric relaxation studies. *J. Mol. Liq.* **301**, 112490 (2020).
14. M.A. Natal-Santiago, M. Hill Josephine, J.A. Dumesic. Studies of the adsorption of acetaldehyde, methyl acetate,

ethyl acetate, and methyl trifluoroacetate on silica. *J. Mol. Catal. A Chem.* **140**, 2 (1999).
15. Y. Zhou, Z. Wang, S. Gong, Z. Yu, X. Xu. Comparative study of hydrogen bonding interactions between N-methylacetamide and methyl acetate/ethyl formate. *J. Mol. Struct.* **1173**, (2018).
16. M.J. Frisch *et al. Gaussian 09, Rev-D.1.* (Gaussian Inc., 2009).
17. A.D. Becke. Density-functional thermochemistry. III. The role of exact exchange. *J. Chem. Phys.* **98**, 7 (1993).
18. C. Lee, W. Yang, R.G. Parr. Development of the Colle–Salvetti correlation energy formula into a functional of the electron density. *Phys. Rev. B.* **37**, 2 (1998).
19. J.G. Moberly, M.T. Bernards, K.V Waynant. Key features and updates for Origin 2018. *J. Cheminform.* **10**, 5 (2018).
20. R. Dennington, T. Keith, J. Millam. *GaussView, Version 6* (Semichem Inc., 2016).
21. W. Humphrey, A. Dalke, K. Schulten. VMD: Visual molecular dynamics. *J. Mol. Graph.* **4**, 1 (1996).
22. T. Lu, F. Chen. Multiwfn: A multifunctional wavefunction analyzer. *J. Comput. Chem.* **33**, 5 (2012).
23. E. Mrazkova, P. Hobza. Hydration of sulfo and methyl groups in dimethyl sulfoxide is accompanied by the formation of red-shifted hydrogen bonds and improper blue-shifted hydrogen bonds: An ab initio quantum chemical study. *J. Phys. Chem. A.* **107**, 7 (2003).
24. A. Jumabaev, H. Hushvaktov, B. Khudaykulov, A. Absanov, M. Onuk, I. Doroshenko, L. Bulavin. Formation of hydrogen bonds and vibrational processes in dimethyl sulfoxide and its aqueous solutions: Raman spectroscopy and ab initio calculations. *Ukr. J. Phys.* **68**, 6 (2023).
25. U. Sherefedin, A. Belay, K. Gudishe, A. Kebede, A.G. Kumela, T.L. Wakjira, K.S. Gizew. DFT and molecular docking analyses of the effects of solvent polarity and temperature on the structural, electronic, and thermodynamic properties of p-coumaric acid: Insights for anti-cancer applications. *Results Phys.* **68**, 108083 (2025).
26. N.A.B. Beigloo, V.H. Rezvan, G. Ebrahimzadeh-Rajaei, A. Shamel. New charge transfer complex between melamine and 4-nitrobenzoic acid: Synthesis, spectroscopic characterization, and DFT studies. *J. Mol. Struct.* **1322**, 140469 (2025).
27. V.H. Rezvan, S.B. Pour, N.J. Behrooz *et al.* A computational perspective on the changes made in the structural, optical, and electronic properties of melamine and picric acid/quinol with the formation of charge transfer complexes. *Struct. Chem.* **1**, 19 (2025).
28. S. Fekadu, A. Kebede, A. Belay, U. Sherefedin, K. Shenkute, D. Tsegaye, Y. Fikre. Investigation of the influence of solvent polarity and temperature on the vibrational spectra, photophysical properties, optical, and thermodynamic characteristics of 1-benzofuran: A density functional theory approach. *J. Solution Chem.* **1**, 34 (2025).
29. U. Sherefedin, A. Belay, K. Gudishe, A. Kebede, A.G. Kumela, T.L. Wakjira, T. Gurumurthi. Effects of temperature and solvent polarity on the thermodynamic and photophysical properties of ferulic acid using density functional theory (DFT). *J. Mol. Liq.* **407**, 125175 (2024).
30. A. Jumabaev, S.J. Koyambo-Konzapa, H. Hushvaktov *et al.* Intermolecular interactions in water and ethanol solution of ethyl acetate: Raman, DFT, MEP, FMO, AIM, NCI-RDG, ELF, and LOL analyses. *J. Mol. Model.* **30**, 349 (2024).
31. A. Jumabaev, B. Khudaykulov, U. Holikulov, A. Norkulov, J. Subbiah, O. Al-Dossary, N. Issaoui. Molecular structure, vibrational spectral assignments, MEP, HOMO-LUMO, AIM, NCI, RDG, ELF, LOL properties of acetophenone and for its solutions based on DFT calculations. *Opt. Mater.* **159**, 116683 (2025).
32. A. Jumabaev, H. Hushvaktov, A. Absanov, B. Khudaykulov, Z. Ernazarov, L. Bulavin. Vibrational spectra and computational study of amyl acetate: MEP, AIM, RDG, NCI, ELF and LOL analysis. *Ukr. J. Phys.* **69**, 10 (2024).

Received 04.09.25

*А. Джумабаєв, Г. Хушвактов,*
*А. Абсанов, І. Дорошенко, Б. Худайкулов,*
*Л. Джуманов, З. Ерназаров*

АНАЛІЗ ВЗАЄМОДІЙ АМІЛАЦЕТАТУ ТА ХЛОРОФОРМУ: КОЛИВАЛЬНА СПЕКТРОСКОПІЯ ТА ДОСЛІДЖЕННЯ КВАНТОВОЇ ТОПОЛОГІЇ

У цьому дослідженні для вивчення спектрального прояву взаємодії між амілацетатом (AmAc) та хлороформом було використано теорію функціонала густини (DFT) та раманівську спектроскопію. Червоний зсув у смузі валентних коливань C=O спостерігався при зменшенні концентрації AmAc у розчині, що свідчить про утворення міжмолекулярних водневих зв'язків у цьому розчині. На рівні DFT/B3LYP/6-311++G(d,p) було визначено оптимальну геометрію комплексів, що складаються з мономера AmAc, димера AmAc та хлороформа. Для збору інформації щодо існування та характеристик водневих зв'язків (таких як C–H···O) було використано методи топологічного аналізу AIM, RDG, NCI, ELF та LOL. Важлива інформація про міжмолекулярні взаємодії в розчині була отримана завдяки відкриттю зв'язку між валентними коливальними смугами C=O та утворенням молекулярних кластерів.

*Ключові слова*: раманівська спектроскопія, водневі зв'язки, амілацетат, хлороформ, поверхня молекулярного електростатичного потенціалу.